MIT Open Access Articles

Artificial Tribotactic Microscopic Walkers: Walking Based on Friction Gradients

Massachusetts Institute of Technology

☙

Artificial Tribotactic Microscopic Walkers: Walking Based on Friction Gradients

Joshua P. Steimel, Juan L. Aragones, and Alfredo Alexander-Katz[*]
Department of Materials Science and Engineering, Massachusetts Institute of Technology, Cambridge, Massachusetts 02139, USA
(Received 10 April 2014; published 22 October 2014)

Friction, the resistive force between two surfaces sliding past each other, is at the core of a wide diversity of locomotion schemes. While such schemes are well described for homogeneous environments, locomotion based on friction in inhomogeneous environments has not received much attention. Here we introduce and demonstrate the concept of tribotaxis, a motion that is guided by gradients in the friction coefficient. Our system is composed of microwalkers that undergo an effective frictional interaction with biological receptors on the substrate, which is regulated by the density of such receptors. When actuated stochastically, microwalkers migrate to regions of higher friction, much like a chemotactic cell migrates to regions of higher chemoattractant concentration. Simulations and theory based on biased random walks are in excellent agreement with experiments. We foresee important implications for tribotaxis in artificial and natural locomotion in biological environments.

Tribotaxis is the process by which an active object, biotic or abiotic, detects differences in the effective local friction coefficient and moves to regions of higher or lower friction according to a given protocol. The local friction coefficient between an object and a surface is dictated by the effective interactions between both. If these interactions are directional in nature, the friction coefficient is anisotropic. A prominent example of this, being the skin of many animals which feels rough when stroked in one direction, yet soft in the other. The origin of this asymmetry is due to the directionality and ordering of hair or scales sticking out from the surface at a slanted angle, which helps in modulating the effective friction between the skin (or scales) of an animal and the surrounding fluid [1,2]. These types of materials are important in many other processes, such as regulating the flow of complex fluids [3], controlling the motion of cells [4], or even skiing up a mountain.

While the motifs that give rise to these asymmetric friction coefficients are rather large, one can envision an alternative microscopic scenario. For example, one can think of exchanging the mechanical texture with a *chemical texture* in which friction is dominated by the strength and spatial density of reversible bonds between an object and a substrate [5,6]. Moreover, gradients in the spatial density of such ligands produce anisotropic friction coefficients. Live cells, for example, naturally detect surface ligand gradients and move accordingly [7]; this is one of the most important clues for locomotion since cells are constantly encountering surfaces in our bodies. Mimicking this behavior using biological ligand-receptor pairs can potentially allow one to "walk on" and sense different conditions in the vast amounts of interfaces in tissues and organs. In addition, chemically based tribotaxis can be used to locally sense friction in purely synthetic environments. Interestingly, despite the tremendous experimental and theoretical effort

in the last years in designing artificial active systems that can perform chemotaxis in an intrinsic way [8–10], the design of a chemotactic artificial active system that detects biological molecules remains a challenge.

Here, we have developed a tribotactic system able to detect gradients in friction due to gradients in the density of biological receptors, thus effectively performing chemotaxis [11–13]. The system is a magnetically assembled colloidal doublet (a microwalker), which converts rotational motion into translational motion due to enhanced friction near a surface. Clearly, for weak friction scenarios the doublet primarily slips and translates slowly while for higher friction coefficients the doublet will *walk* faster in a hinge-type fashion [see Fig. 1(a)]. The effective friction for this system can be tuned by functionalizing the surface of the magnetic beads and the substrate with complementary ligand-receptor pairs [Fig. 1(b)]. Thus, by controlling the spatial density of ligands on the surface it is possible to create gradients in the friction coefficient. From nonequilibrium mechanics, it is known that if a particle is stochastically driven on such gradients, its motion resembles that of biased random walks [14]. To create such stochastic walks, we utilize a particular protocol that can be best described in a two-part scheme per random step. In the first part, the so-called move step, we rotate the microwalker by applying a torque in a given direction for a fixed time τ. In the second part, the so-called relax step, we allow the doublet to lie flat for a period of time τ_{relax}, which increases the probability of forming bonds with the substrate. We repeat this protocol for the total number of steps of the walk and randomize the direction of the torque per step according to a one-dimensional random walk. Clearly, over the course of multiple steps following the protocol previously described, the microwalker will drift toward regions of higher ligand density where friction is higher, eventually becoming trapped in such regions.
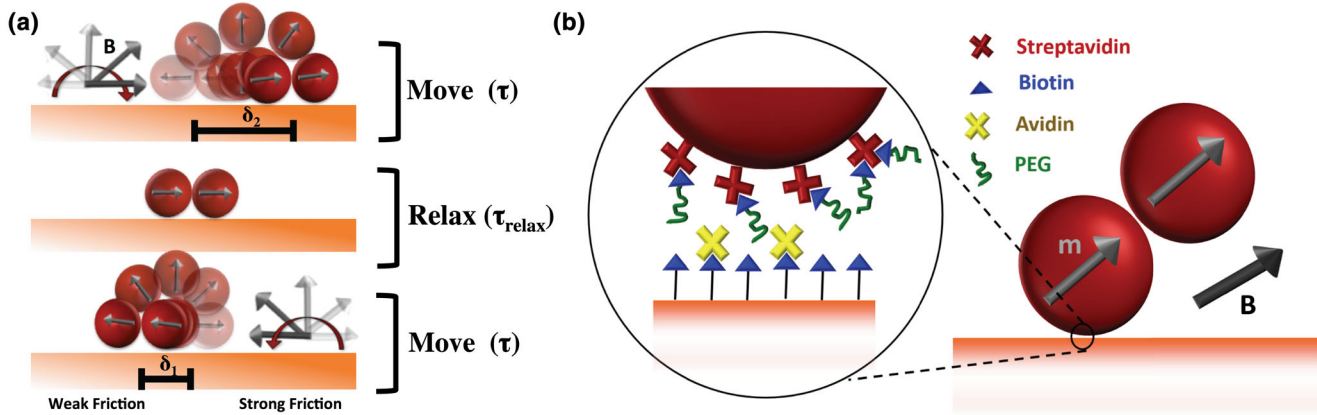
FIG. 1 (color online).   Schematic representation of the tribotactic system. (a) A superparamagnetic doublet, or microwalker, spontaneously self-assembles upon actuation of the magnetic field, B. To rotate the magnetic doublet on the substrate we couple the doublet to a rotating magnetic field. The microwalker is actuated for a time period τ and is then allowed to relax for a certain period τ_{relax}; this constitutes one random walk step. The motion of the center of mass of the tribotactic walkers is, in general, denoted by δ. In particular, the walkers tend to perform larger displacements δ_2 when moving toward regions of higher friction and display smaller steps toward regions of lower friction δ_1. Hence, the microwalker will drift toward regions of higher friction, effectively migrating toward areas with a higher ligand density. (b) The effective friction (or interaction) between the beads and the substrate is controlled by functionalizing both surfaces with complementary ligand-receptor pairs. In this Letter the beads are functionalized with streptavidin and the substrate with biotin. The beads, 3 μm in diameter, are further functionalized with biotinylated polyethylene glycol (mPEG-biotin) to mask and reduce the effective binding strength between the walker and the substrate. Free avidin is also used to block available binding sites on the substrate.

As mentioned above, our tribotactic system is composed of two superparamagnetic beads coated with streptavidin and a biotinylated substrate. To modulate the surface and reduce the binding strength of the biotin-streptavidin bond, we decorate such beads with biotinylated PEG, leaving only a few active sites on the surface. The density and distribution of available biotin sites on the substrate can also be screened by using free avidin [see Fig. 1(b)]. The gradients in friction were created by drying a water droplet (50 μl) containing free avidin ligands at a concentration of 1 mg/ml and left to evaporate on a biotinylated substrate [see Fig. 2(a)]. The capillarity flows induced by the differential evaporation rates across the droplet carry most of the avidin ligands to the edge, thereby producing a so-called coffee-ring pattern along the perimeter of the droplet [15]. Interestingly, a robust annular friction pattern develops around the center of the droplet [see Fig. 2(b)]. Notice that such patterns have also been observed in other evaporating systems [16]. The resulting frictional landscape exhibits areas of high friction separated by low friction "valleys." This can be seen in Fig. 2(c), where we plot the velocity of translation of the doublet vs the distance to the center of the droplet. In this case we continuously allow the microwalker to move, effectively setting $\tau \to \infty$. Note that higher velocities correspond to higher effective friction. In particular, we find the velocity at $x \approx 0$ μm and $x \approx 800$ μm to be approximately 30–40% larger than at the lowest point, corresponding to $x = 450$ μm. The velocity displayed in this latter region corresponded to a biotin substrate that was completely coated with avidin ligands

(the horizontal red dashed line), which was confirmed by an independent measurement on a surface with no free biotin (Fig. S4a [17]). Assuming a simple Stokes drag scenario, the variations in velocity imply a difference in effective friction forces between both regions of less than 60 fN. Thus, our microwalkers are extremely sensitive to minute variations in the friction coefficient. For more details about the system, the materials, and the methods we refer the reader to the Supplemental Material [17].

The tribotactic nature of our microwalkers was probed by actuating them with a rotating magnetic field where the direction of rotation is varied in a stochastic fashion, as in a one-dimensional random walk. The total number of steps in each walk is set to 300, and we allow the system to relax for $\tau_{\text{relax}} = 10$ s in between steps, which provides enough time for the doublet to lie parallel to the substrate. The period of actuation, τ, was set at 2 s. In Fig. 3(a), the trajectories for several independent random walks originating from different points in the sample are plotted. As is clear from this plot, the doublets initially positioned at $x = 0$ and $x = 800$ μm become *trapped* in these regions with a larger friction coefficient. Walkers initially positioned at regions with a lower coefficient of friction, like $x = 300$ and $x = 600$ μm, drift along the gradient in the direction of stronger friction. The region with the lowest friction is at an unstable point and the microwalkers can go either way. This is clearly observed for the walkers initially positioned around $x = 450$ μm, which drifted in both directions [see green trajectories in Fig. 3(a)]. For microwalkers starting at $x = 300$ μm and $x = 600$ μm, we
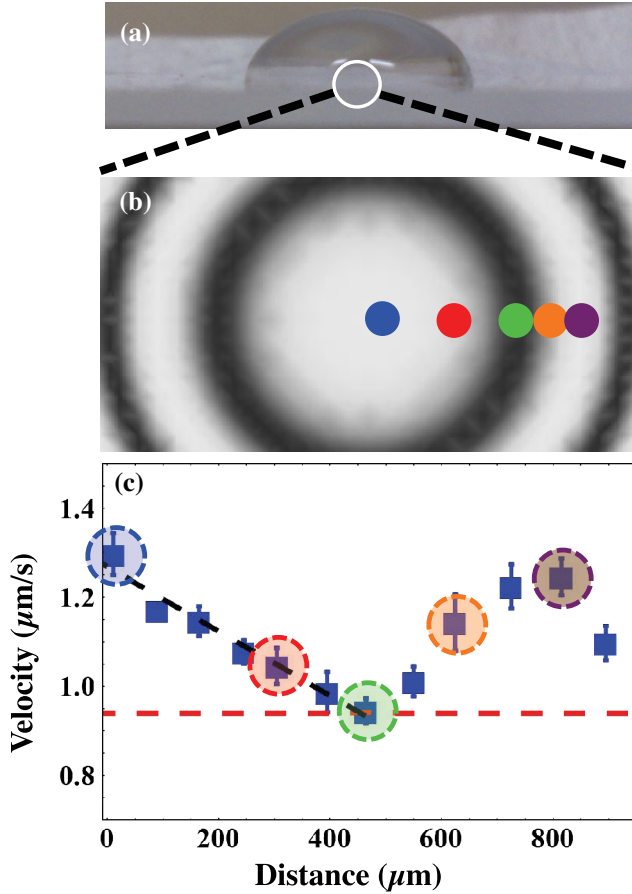
FIG. 2 (color online). Creating gradients in the density of biotin binding sites and mapping the velocity profile of the substrate. (a) A water droplet containing avidin is placed on the biotinylated substrate and left to evaporate for 24 hrs. (b) Schematic of the gradient in the density of available biotin binding sites based on the frictional landscape obtained by measuring the local walking velocities shown below. (c) Average velocity profile (μm/s) of the microwalkers as a function of the distance to the center of the droplet in μm. The origin ($x = 0$ μm) corresponds to the center of the avidin droplet. The horizontal red line denotes the velocity of the walkers on a fully passivated biotin surface, measured in an independent experiment. The colored dots denote the initial positions from which the random walks in Fig. 3 were launched. The frequency of rotation is set to 1 Hz.

computed the drift velocity from the slope of a linear fit to their trajectories [see Figs. 3(b) and 3(c)]. The drift was estimated to be $u = 0.32$ μm/s ($x = 300$ μm) and $u = 0.28$ μm/s ($x = 600$ μm). Notice, however, that the drift velocity of these tribotactic microwalkers can be tuned by modifying the parameters of the system, such as the actuation protocol or the size of the walkers. Furthermore, our approach is extremely versatile because the beads can be functionalized with a multitude of biologically relevant motifs or can even be multiplexed, meaning they can have combinations of motifs to explore cooperative effects or multiple gradients. Thus, such tribotactic microwalkers can

be used as sensitive chemotactic probes in biological environments. Notice that the origin of the tribotactic response in our system is due to the frictional landscape of the environment and not on the presence of a (non-biological) fuel source [10,18,20], and thus the chemotactic landscape is static. Hence, our tribotactic walkers complement current approaches to create artificial chemotactic systems.

To further understand our tribotactic system, we analyzed the distances traveled by the walkers at each step for both directions. A probability distribution of such displacements is shown in the insets of Figs. 3(b) and 3(c) for the doublets positioned at $x = 600$ μm and $x = 300$ μm, respectively. From these distributions it is clear that the tribotactic walkers exhibit, on average, asymmetric displacements depending on the direction of motion. The average displacement toward regions with weaker friction is denoted by $\delta_1(x)$ and toward regions with stronger friction is denoted as $\delta_2(x)$, and their corresponding standard deviations are $\sigma_1(x)$ and $\sigma_2(x)$ (see insets in Fig. 3). It is well known that such asymmetric distributions lead to directed motion (drift). In order to see this, one can develop a master-equation-based model of the stochastic motion exhibited by the doublets that incorporates such distributions of microscopic displacements. By deriving a *Fokker-Planck* equation via a truncated *Kramers-Moyal* expansion of the original *master equation* [21], it is possible to solve the time evolution of the probability distribution of the position of the walkers. This model equation has previously been used to describe chemotaxis [22–26]. Note that the actuation protocol is that of a random walk and thus has no memory. The model and subsequent derivation of the governing equations can be found in the Supplemental Material [17]. The final equation that describes the temporal evolution of the probability density is given by

$$\frac{\partial P(x,t)}{\partial t} = -\frac{\partial}{\partial x}[u(x)P(x,t)] + \frac{1}{2}\frac{\partial^2}{\partial x^2}[D(x)P(x,t)], \quad (1)$$

where $u(x)$ and $D(x)$ are the drift velocity and diffusion coefficient of the walkers, respectively. These coefficients have a microscopic origin, and their functional form can be written in terms of the displacements $\delta_1(x)$ and $\delta_2(x)$ as $u(x) = (\delta_2(x) - \delta_1(x))/\tau$ and $D(x) = (\delta_1(x)^2 + \delta_2(x)^2) + (\sigma_1(x)^2 + \sigma_2(x)^2)/\tau$. The first term is responsible for tribotactic motion and represents the drift due to the asymmetry in displacements, while the second term corresponds to diffusive motion. Assuming the magnitude of the displacements is independent of the position (i.e., $u = $ constant), which is the case we find experimentally (see Fig. S6b [17]), the solution to Eq. (1) is a normal distribution whose average drifts with time at a velocity u, and the width of the distribution grows as $t^{1/2}$. Such growth can be better seen from simulated random walks with
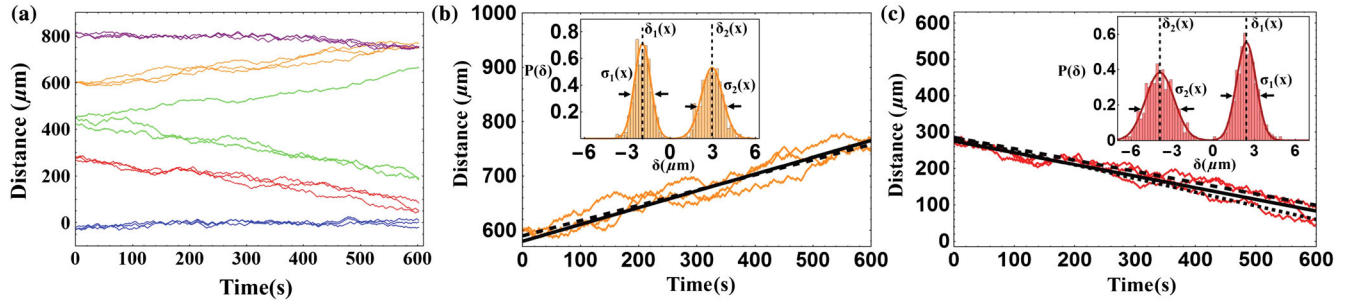
FIG. 3 (color online).   Trajectories of tribotactic microwalkers driven stochastically. (a) Random-walk trajectories for doublets initially placed at approximately 0, 300, 450, 600, and 800 μm from the origin. The color of the walk corresponds to the highlighted position in Fig. 2(c). A drift toward regions with a higher friction coefficient is observed. Walkers initially placed in regions with the maximum friction coefficient became trapped. (b) Detailed trajectories for walkers initially placed at 600 μm. The solid, dashed, and dotted lines correspond to a linear fit to the experimental trajectories (slope 0.28 μm/s), the simulated trajectories, and the theoretical drift velocity $(u = [\delta_2(x) - \delta_1(x)]/\tau)$, respectively. (Inset) Probability distribution of the displacement in each direction. $\delta_1(x)$ corresponds to the mean displacement in the direction of lower friction, while $\delta_2(x)$ denotes the average displacement toward higher friction areas. (c) Trajectories for walkers initially placed at 300 μm. $\delta_1(x)$ and $\delta_2(x)$ are defined as in part B. The different lines correspond, as in part B, to the linear fits to the experimental (solid line), simulated (dashed line), and theoretical (dotted line) results. The slope of the linear fit to the experimental data is 0.32 μm/s.

displacements distributed according to those found experimentally (see Fig. S5 [17]). The drift velocities from such simulated experiments are in excellent agreement with the theoretical and experimental values, as can be seen by comparing the dashed (simulated trajectories), dotted (analytical model), and solid (experimental trajectories) lines in Figs. 3(b) and 3(c).

As described above, the regions of highest friction act as *tribotactic traps*. To measure the relative strength of these traps with respect to the spatial step size of the random walks, we performed longer stochastic sequences of 500 steps starting at the center of the trap. The effective spatial step size was varied by changing the actuation period, τ, of the rotating magnetic field from 2 to 20 s. The resulting trajectories were analyzed, and the corresponding probability distributions are presented in Figs. 4(a) and S7a [17]. The solid lines in Fig. 4(a) represent the numerical solutions based on Eq. (1) of our tribotactic model, including the directional dependence of the drift term due to the trap [17]. We also simulated many more repetitions of such random walks to get better statistics [17]. As expected, the increase in τ translates into a broadening of the steady-state distributions. In light of the Gaussian-like shape of the steady-state distribution, we evaluated the stiffness of the trap κ using the standard deviation, σ, of such distribution from Fig. 4(a). From statistical mechanics we know that the probability distribution of an harmonic oscillator can be written as $P(x) \propto \exp\left(-\frac{1}{2}\kappa(\tau)x^2\right)$, where $\kappa = 1/\sigma^2$. In Fig. 4(b) we can see that $\kappa \propto 1/\tau^2$; thus, τ plays the role of a square root of a temperature by analogy to the simple harmonic well. To corroborate the results from the steady-state distributions, we calculated also the root-mean-square displacement (RMSD) for the trajectories. As expected, the RMSD, for both simulations and

experiments, exhibits a plateau at long times for all of the different τ. Such behavior is characteristic of a confined random walker and directly corroborates the presence of a tribotactic trap.
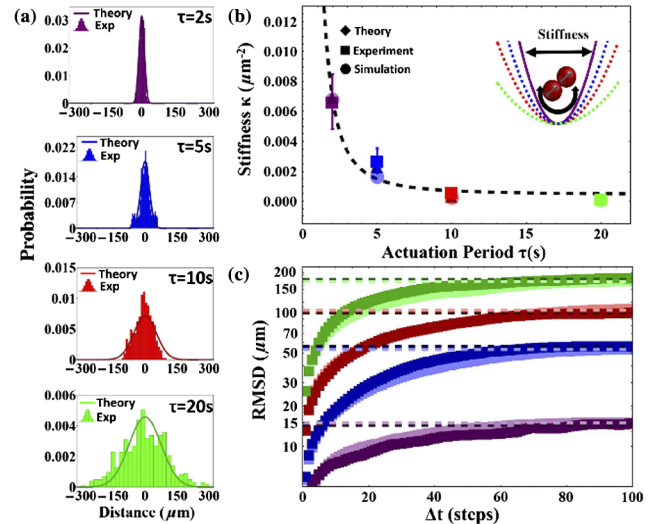

FIG. 4 (color online).   Tribotactic trap. (a) Experimental probability distribution of position of tribotactic walkers with an actuation period, τ, of 2 s (purple), 5 s (blue), 10 s (red) and 20 s (green), respectively. Solid lines correspond to the numerical solutions to Eq. (1) using the experimental parameters for the step displacement distribution. (b) *Stiffness* of the tribotactic trap, κ, computed from the standard deviation of the distributions obtained experimentally (squares), using simulations (circles), and using the analytical model (diamonds). The dashed line represents a fit to the data assuming the functional form $\kappa \propto \tau^{-2}$. (c) RMSD calculated from the experimental (darker colors) and simulation (lighter colors) trajectories for actuation periods of 2 s (purple), 5 s (blue), 10 s (red) and 20 s (green). The RMSDs show the characteristic behavior of a confined random walk.

In summary, we have demonstrated tribotaxis using a superparamagnetic doublet functionalized with biological ligands. Such a microwalker exploits friction to sense ligand concentration gradients and migrates toward the higher density regions, eventually becoming trapped in such regions. To avoid trapping, we have shown that increasing the actuation time yields a "softening" of the trap and can in principle lead to escape, similar in spirit to the way bacteria escape from their own chemoattractant [27]. Thus, the frictional landscapes felt by these tribotactic microwalkers can be tuned, making this system ideal to measure differences in friction coefficients in complex environments or to find areas with relatively higher density of ligands without *a priori* knowledge. Furthermore, given the similarities between cells and the aforementioned microwalkers in terms of size and the environment in which they move, we believe that nature may already be using friction as an ultrasensitive probe for differences in the density of ligands which ultimately play a determining role in biological processes.

[*]aalexand@mit.edu

[1] G. D. Bixler and B. Bhushan, Soft Matter **8**, 11271 (2012).

[2] J. Hazel, M. Stone, M. S. Grace, and V. V. Tsukruk, J. Biomech. **32**, 477 (1999).

[3] D. Quéré, Annu. Rev. Mater. Res. **38**, 71 (2008).

[4] M. Le Berre, Y.-J. Liu, J. Hu, P. Maiuri, O. Bénichou, R. Voituriez, Y. Chen, and M. Piel, Phys. Rev. Lett. **111**, 198101 (2013).

[5] J. Klein, Annu. Rev. Mater. Sci. **26**, 581 (1996).

[6] B. Bhushan, J. N. Israelachvili, and U. Landman, Nature (London) **374**, 607 (1995).

[7] S. B. Carter, Nature (London) **213**, 256 (1967).

[8] S. Granick, S. K. Kumar, E. J. Amis, M. Antonietti, A. C. Balazs, A. K. Chakraborty, G. S. Grest, C. Hawker, P. Janmey, E. J. Kramer, R. Nuzzo, T. P. Russell, and C. R. Safinya, J. Polym. Sci., Part B: Polym. Phys. **41**, 2755 (2003).

[9] A. Bhattacharya, O. B. Usta, V. V. Yashin, and A. C. Balazs, Langmuir **25**, 9644 (2009).

[10] S. J. Ebbens and J. R. Howse, Soft Matter **6**, 726 (2010).

[11] H. C. Berg and D. A. Brown, Nature (London) **239**, 500 (1972).

[12] J. Alder, Science **153**, 708 (1966).

[13] H. C. Berg, Annu. Rev. Biophys. Bioeng. **4**, 119 (1975).

[14] E. A. Codling, M. J. Plank, and S. Benhamou, J. R. Soc. Interface **5**, 813 (2008).

[15] L. Shmuylovich, A. Q. Shen, and H. A. Stone, Langmuir **18**, 3441 (2002).

[16] D. Kaya, V. A. Belyi, and M. Muthukumar, J. Chem. Phys. **133**, 114905 (2010).

[17] See Supplemental Material at http://link.aps.org/supplemental/10.1103/PhysRevLett.113.178101, which includes Refs. [14–16,18,19,22], for a more detailed description of the experimental protocol, data analysis and the analytical model.

[18] W. F. Paxton, K. C. Kistler, C. C. Olmeda, A. Sen, S. K. St Angelo, Y. Cao, T. E. Mallouk, P. E. Lammert, and V. H. Crespi, J. Am. Chem. Soc. **126**, 13424 (2004).

[19] E. W. Montroll and M. F. Shlesinger, in *On the Wonderful World of Random Walks*, edited by J. L. Lebowitz and E. W. Montroll (North-Holland, Amsterdam, 1984).

[20] J. R. Howse, R. A. L. Jones, A. J. Ryan, T. Gough, R. Vafabakhsh, and R. Golestanian, Phys. Rev. Lett. **99**, 048102 (2007).

[21] N. G. Van Kampen, *Stochastic Processes in Physics and Chemistry* (Elsevier, New York, 2011).

[22] J. S. Guasto, R. Rusconi, and R. Stocker, Annu. Rev. Fluid Mech. **44**, 373 (2012).

[23] E. F. Keller and L. A. Segel, J. Theor. Biol. **30**, 225 (1971).

[24] W. Alt, J. Math. Biol. **9**, 147 (1980).

[25] R. B. Dickinson and R. T. A Tranquillo, J. Math. Biol. **31**, 563 (1993).

[26] G. Maheshwari and D. A. Lauffenburger, Microsc. Res. Tech. **43**, 358 (1998).

[27] Y. Tsori and P.-G. de Gennes, Europhys. Lett. **66**, 599 (2004).